International Journal of Nanoelectronics and Materials

In Press, Accepted Manuscript – Note to users

Synthesis and Characterization of Zinc Oxide Nanoparticles using Green and Chemical Synthesis Techniques for phenol decontamination

H. Shokry Hassan[1*], M. F. Elkady[2,3], E.M. El-Sayed [3] A. M. Hamed[4], A. M. Hussein[4], Islam M. Mahmoud[4]**

[1]Electronic Materials Researches Department, Advanced Technology and New Materials Research Institute, City of Scientific Research and Technological Applications, New Borg El-Arab, 21934, Alexandria, Egypt. Email: hassan.shokry@gmail.com

[2]Chemical and Petrochemical Engineering Department, Egypt-Japan University of Science and Technology, New Borg El-Arab, Alexandria, Egypt. Email: marwa.f.elkady@gmail.com

[3]Fabrication Technology Researches Department, Advanced Technology and New Materials Research Institute, City of Scientific Research and Technological Applications, New Borg El-Arab, 21934, Alexandria, Egypt.

[4]Chemistry Department, Faculty of Science Al-Azhar University, Al-Azhar uni Street, 71524 Assiut, Egypt.

Abstract

Zinc oxide nanoparticles (ZnO-NPs) were successfully synthesized using both biological and chemical techniques. This study, mainly focused on green synthesis (biological) method of ZnO-NPs using different plant leaves extract such as (guava, olive, fig and lemon). The plant leaves extract (polyphenols) act as reductant and zinc nitrate hexahydrate ($Zn(NO_3)_2.6H_2O$) as precursor. Chemical synthesis method of ZnO-NPs was prepared using sodium hydroxide and zinc nitrate. The produced ZnO-NPs were characterized using X- ray diffraction (XRD), scanning electron microscope (SEM), transmission electron microscopy (TEM), fourier transform infrared (FTIR), Thermal gravimetric analysis (TGA), and particle size analysis (PSA). The average crystallite size of green synthesized zinc oxide nano powders ranged from 7.1 to 28 nm, while the average crystallite size of chemical synthesized zinc oxide powders ranged from 19.6 to 148 nm according to the XRD calculations and TEM observations. Both ZnO nanopowders showed high thermal stability up to 600 ^oC. The green synthetized ZnO-NPs was evaluated for phenol decontamination from polluted wastewater. The maximum recorded phenol removal was 99.7% within 250 minutes using 0.1g ZnO-NPs. So, ZnO-NPs represent promising adsorbent material for phenol decontamination from polluted wastewater.

Keywords: Zinc oxide nanoparticles (ZnO-NPs); Green synthesis; Biological and Chemical synthesis; Plant leaves extract; phenol removal.

In Press, Accepted Manuscript – Note to users

1. Introduction

The growth and development of mankind has always been closely associated with the progress of materials technology. In the last decades, the field of nanotechnology and the associated researches was continuously in high growth due to the experience and the capitalization of accumulated knowledge [1]. A large variety of nanomaterials have attracted more consideration because of their desirable properties and the possibility to use in innovative technology applications [2,3]. A nanoparticle can be defined as a small object that acts as a whole unit in terms of its transport and properties. The engineering and science technology of nano-systems are considered the most demanding and rapid growing areas of nanotechnology. Physical and chemical processes are more convenient for nanoparticle synthesis whoever; the use of toxic compounds restricts their application [4].

Zinc oxide has been an essential material for industry for centuries and is presently the subject of significant new interest. ZnO is a white powder that is insoluble in water, which is already widely used in our society as an additive in numerous materials and products, and indeed it is a key element in many industrial manufacturing processes but most zinc oxide is prepared synthetically [5]. It is well known that the sizes, phases and morphologies of the nanomaterials have a large impact on their properties and technological applications. Therefore, many researchers have focused in there researches on the control of morphological structures of nanomaterials [6].

Biosynthesis of nanoparticles has gained significant importance in recent years and has become one of the most preferred [7-9]. In biosynthesis method f ZnO NPs, plant leaves extract are used for controlled and e synthesis of zinc oxide nanoparticles using the aqueous extract of different plant leaves as reductant to develop an environmentally friendly process through biomimetic approaches rather than traditional methods using various routes for the synthesis of ZnO NPs. These techniques in general, can be divided into three kinds that is chemical, physical and biologically methods. Chemical synthesis can be further divided into liquid and gas phase synthesis. Liquid phase synthesis includes but limited for the following methods; precipitation, coprecipitation method [10], colloidal methods, sol-gel processing [11], water–oil microemulsions method [12], hydrothermal synthesis [13], solvothermal, sonochemical [14], polyol method [15] and vapor phase [16]. Fabrication includes pyrolysis, inert gas condensation methods and laser ablation are classified as physical methods [17]. However, all these mentioned techniques are extremely expensive and have many disadvantages due to the

difficulty of scale up the process of synthesis, separation and purification of nanoparticles from the surfactants, co-surfactants, organic solvents, and toxic materials which involve use of toxic, hazardous chemicals like borohydride, hydrazine hydrate, citrate and hydrazine hydrochloride as reductants.

Phenols are considered one from the top 45th importance risky substances that required being treated before its release into the environment that referring to Agency for Toxic Substances & Dis- ease Registry, USA classification. Indeed, even at low concentration, phenols have a murder and decimating effect on the life form such as sour mouth, diarrhea, impaired vision, and excretion of dark urine [18].

Recently, growth awareness towards green chemistry and other biological processes have led to the improvement of rapid, cost-effective and an eco-friendly environmentally biosynthesis of zinc oxide Nano powder using plant leave extracts approach for the synthesis of nanoparticles [19].This investigation compare between the physico-chemical properties of ZnO nano powder materials produced from both chemical and biological routes.

2. Material and methods

2.1. Materials

High pure grades of Zn $(NO_3)_2.6H_2O$ and NaOH were supplied from Sigma-Aldrich chemicals. Plant fresh leaves of guava, olive, fig and lemon were collected early in the morning during the month of May 2016 from Sohag – Egypt.

2.2. Extraction of the antioxidants (poly phenols) from plant leaves

Preparation of plant leaves extract were collected from different Fresh plant leaves of olive, Preparation of plant leaves extract were collected from different Fresh plant leaves of olive, guava, fig and lemon. These leaves were collected and washed with water and distilled water for dust removal and then dried overnight at oven at 70°C. The leaves after drying were grinded into fine powder. The extract was utilized for the reduction of zinc ions (Zn^{2+}) to (ZnO) nanoparticles that was prepared by placing 12.5g of dried leaves in 250ml beaker with 200ml water. The mixture was then boiled for 2 hours at 60-80˚C using a stirrer heater until the colour of the aqueous solution changes from watery to light yellow. The extract cooled to room temperature and filtered using filter paper. The extracted filtrate was stored at refrigerator and utilized as reducing agent [20].

2.3. Synthesis of ZnO nanoparticles

ZnO NPs was prepared using two techniques, chemically and green synthesis using sodium hydroxide and plant leaves extract collected from different Fresh and dry plant leaves of olive, guava, fig and lemon respectively.

2.3.1. Biosynthesis of ZnO nanoparticles

In this method the liquid extract of the antioxidants (poly phenols) from plant leaves was utilized for zinc salt reduction. 70 ml of $Zn(NO_3)_2.6H_2O$ with concentration of 0.2 M was reduced with 30 ml from (Olive, guava, fig and lemon) leaves extract (stored at refrigerator) . These extracts were added under constant stirring, dropwise and boiled to 60˚C using a stirrer-heater for 1hr. The produced powder materials were dried at 100°C overnight. During the drying process, complete conversion of zinc hydroxide into zinc oxide takes place until its color converted into darck yellow colored paste. This paste collect in a ceramic crucible and calcinated at 500˚C for 2 hours. A sunny yellow powder was produced after calcination process. The material was grinded after calcination to produce fine powder. The schematic diagram of ZnO Biosynthesis method showed in (**Figure1**) [20,21].

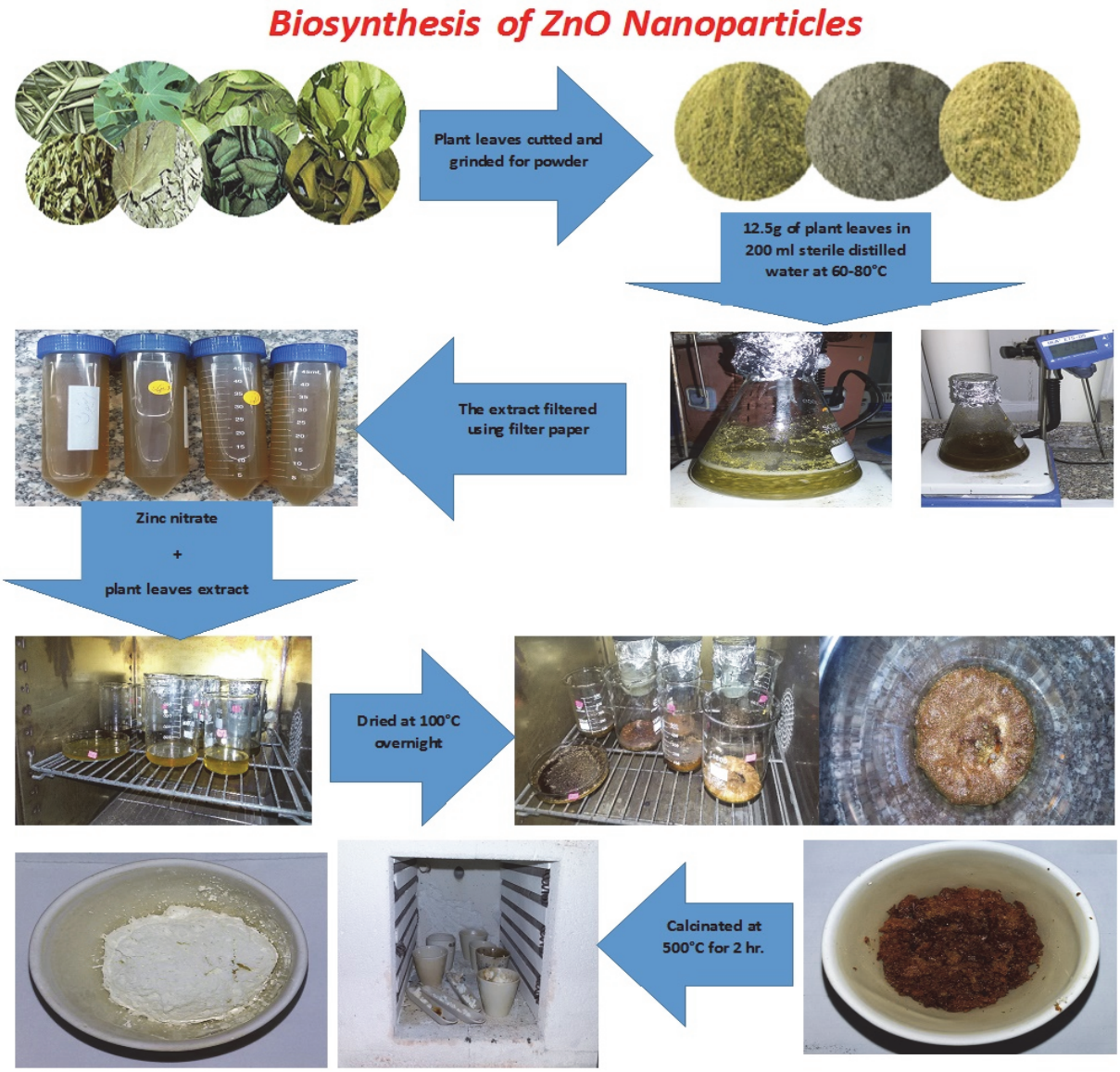

Figure 1. Biosynthesis of ZnO nanoparticles schematic diagram

2.3.2. Chemical Synthesis of Zinc Oxide nanoparticles

The sol-gel technique as most facile method was utilized for zinc salt reduction. The solution of $Zn(NO_3)_2.6H_2O$ at concentration 0.2 M was reduced using 9.8 ml of 2 M sodium hydroxide. The reducing agent was added dropwise under constant stirring until solution pH reach 12. After complete addition of NaOH the reaction continued for 2 hr. The solution reaction was kept overnight and the produced solid materials were separated using centrifugation force. The separated powder material was washed using distilled water. Finally, the material was dried at 100°C. During the drying process, the conversion of zinc hydroxide into ZnO was take place [22].

2.4. Characterization of the Prepared Zinc Oxide nanoparticles

X-ray diffraction patterns of the nanopowders were obtained using (Schimadzu 7000) Diffractometer operating with Cu Kα radiation (λ = 0.15406nm). Generated at 30kV and 30mA with scan rate of 2° min^{-1} for 2θ values between 20 and 80 degrees. Scanning electron microscopic SEM analysis (JEOL JSM 6360LA, Japan) were performed to determine the shape and morphology of ZnO nanoparticle. The morphologies and size of prepared ZnO materials were detected using TEM (JEOL JEM 1230, Japan). FTIR spectrums of prepared ZnO materials were established using (Shimadzu FTIR-8400 S, Japan) at wave length range 400 – 4000 cm^{-1}. The thermal stability of ZnO prepared was evaluated by Thermo gravimetric analysis (TGA) using Thermo gravimetric Analyzer (ShimadzuTGA–50H, Japan), the particle size of ZnO material and its distribution were determined using particle size analyzer (PSA) (LA-960 combines).

2.5. Assessment of the green synthetized ZnO-NPs for phenol sorption

The affinity of the green synthetized ZnO-NPs toward phenol sorption was verified using synthetic polluted water in batch manner. The phenol sorption profiles of 0.1 g of green synthetized ZnO-NPs were determined against the contact time (0-250 min). The percentage removal of phenol using tested ZnO-NPs was estimated from "Eq. (1)"

$$\% \text{ Removal} = ((C_o - C) / C_o) * 100 \quad (1)$$

where C_o is the initial phenol concentration in solution (mg/l), and C is the final phenol concentration after treatment process (mg/l).

3. Results and discussion

The end product of zinc oxide nanoparticles were successfully synthesized using green synthesis method in a light yellow colored powder precipitate, however that prepared using chemical synthesis method represent a white precipitate.

Bio-reduction of the zinc ions (Zn^{2+}) to ZnO during exposure to the plant leaf extracts was followed by color change from pale yellow to yellowish brown color after the drying process. On the other side in chemical synthesis method, zinc salt was reacted with sodium hydroxide to produce zinc hydroxide and sodium nitrate. This hydroxide decomposes upon heating to zinc oxide. Both green and chemical preparation techniques of ZnO nanomaterials depend on a spontaneous reduction of zinc salt "Eq. (2), (3)".

$$Zn(NO_3)_2 + 2NaOH \rightarrow Zn(OH)_2 + 2NaNO_3 \quad (2)$$

$$Zn(OH)_2 \rightarrow ZnO + H_2O \quad (3)$$

During $Zn(OH)_2$ decomposes into ZnO nanoparticles. The yield obtained was 1.6 g which means about 60% of precursor used was converted into pure ZnO nanoparticles in green synthesis method. However, this production yield of ZnO nanoparticles was increased to 87% using chemical preparation technique.

3.1. XRD Analysis

XRD was used to characterize the different methods of the prepared ZnO nanopowders. **Figure 2** shows XRD pattern for ZnO nanopowder synthesized by both chemical and green techniques using extracts from different Fresh and dry plant leaves of olive, guava, fig and lemon. X-ray diffraction of the Zinc oxide NPs synthesized by chemical method using zinc nitrate and sodium hydroxide was investigated at **Figure 2** (A) it was indicated from this figure that distinctive peaks were appeared at (100), (002), (101), (102), (110), (103), (200), (112) and (201). The results confirmed that the prepared ZnO nanoparticles are of wurtzite hexagonal structure and showed high degree of crystallinity.

The X-Ray powder Diffraction pattern of the synthesized sample from aqueous plant leaves extract by Green synthesis method was illustrated at **Figure 2** (B_1, B_2, C_1, C_2, C_3, C_4). It was indicated distinctive peaks appear at (100), (002), (101), (102), (110), (103), (200), (112) and (201), that are in good agreement with wurtzite ZnO (JCPDS CARD NO: 36- 1451) [23]. The X-ray pattern clearly demonstrated that all diffraction peaks of the prepared ZnO NPs have high purity and high degree of crystallinity structure. The X-ray diffraction peaks clearly demonstrated that the pattern of fresh and dry plant leaves extract has ability to green synthesized ZnO NPs that have the same diffraction peaks without any changes. The sharp and narrow diffraction peaks indicate that the product is well crystalline in nature. The mean crystalline size (D) of the particles was determined from the XRD line broadening measurement using Scherrer equation "Eq. (4)"

$$D=0.89\lambda / (\beta \text{Cos}\theta) \quad (4)$$

Where D is the mean size of crystallites (nm), K is the Scherrer constant crystallite shape factor a good approximation is 0.9, λ represents wavelength of x-ray source (Cu Kα) 0.1541 nm used in XRD, B is full width at half the maximum of the diffraction peak (FWHM) in radians of the X-ray diffraction peak and θ is the Bragg (diffraction) angle. The XRD peaks were not as sharp as in the case of chemical synthesis method sample when compared with green synthesis method, it means that the slight decrease in crystallinity, which suggests the formation of smaller particle size. The calculated average crystalline size of zinc oxide nano particles

prepared from chemical synthesis method was calculated as 19.6 nm, while The size reduced to 8.5, 9.49, 7.10, 10.34, 9.3 and 13.76 nm respectively when chemical synthesis was replaced by green synthesis using extracts from different Fresh and dry plant leaves of olive, guava and dry plant leaves extract of fig and lemon respectively. It can be clearly seen that the broadening of peaks in green synthesis using extracts of olive, guava and dry plant leaves extract of fig and lemon are greater compared to the chemical synthesis method, indicating that the particles synthesized by green synthesis have a smaller particle size [24, 25].

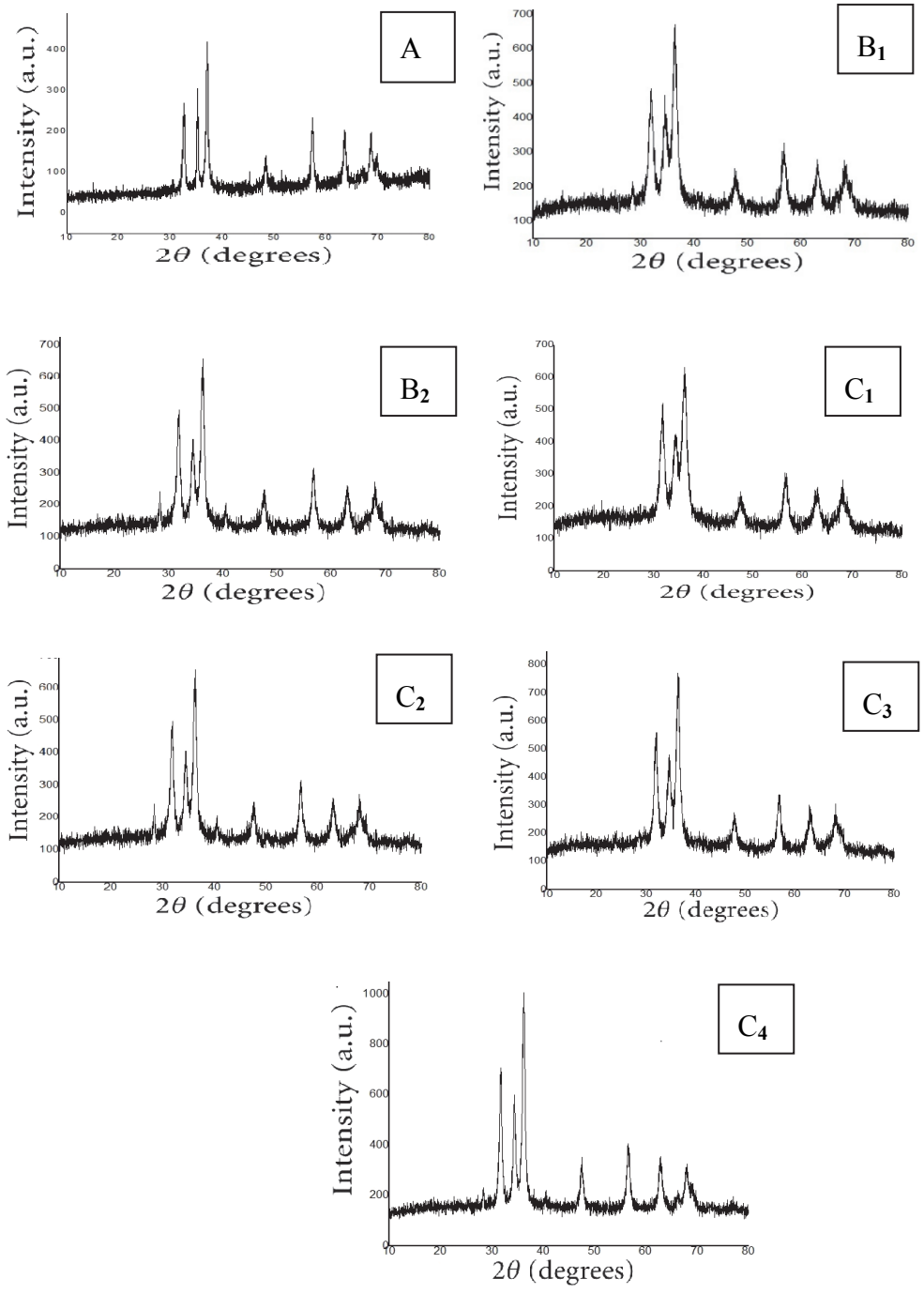

Figure 2 XRD spectrums of synthesized pure nano zinc oxide using both chemical and green synthesis methods: (A) chemical, (B_1) olive fresh, (B_2) guava fresh, (C_1) olive dry, (C_2) guava dry, (C_3) fig dry and (C_4) lemon dry.

3.2. SEM Analysis

The scanning electron microscopic (SEM) analysis was performed to determine the shape and morphology of pure ZnO nanoparticle under various magnifications and results were depicted in the **Figure 3**. The SEM results of studies Zinc Oxide Nanoparticles synthesized using both chemical and green synthesis methods using extracts from different Fresh and dry plant leaves of olive, guava, fig and lemon revealed the formation of stable Zinc oxide nanoparticles, In this study SEM image has showed spherical, spongy and irregular shape of ZnO nanoparticles, In addition to individual zinc particles as well as a number of aggregates, Respectively. The SEM image (**Figure 3**) showed that the particle size of green synthesized zinc oxide nanoparticles (**Figure 4** from B_1-C_4) were comparatively less than that of the chemical synthesized nanoparticles (**Figure. 3** A) and the particle size of fresh green synthesized spherical shape zinc oxide nanoparticles (**Figure 3** B_1, B_2) were comparatively less than that of dry green synthesized irregular and spongy zinc oxide nanoparticles (**Figure 3** C_1, C_2, C_3, C_4). These results have good agreement with XRD results [21].

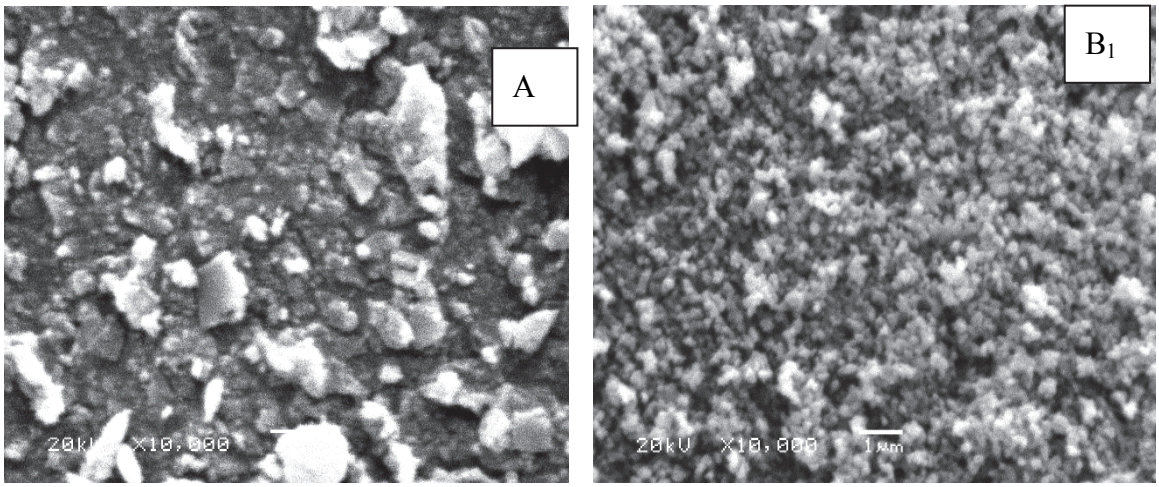

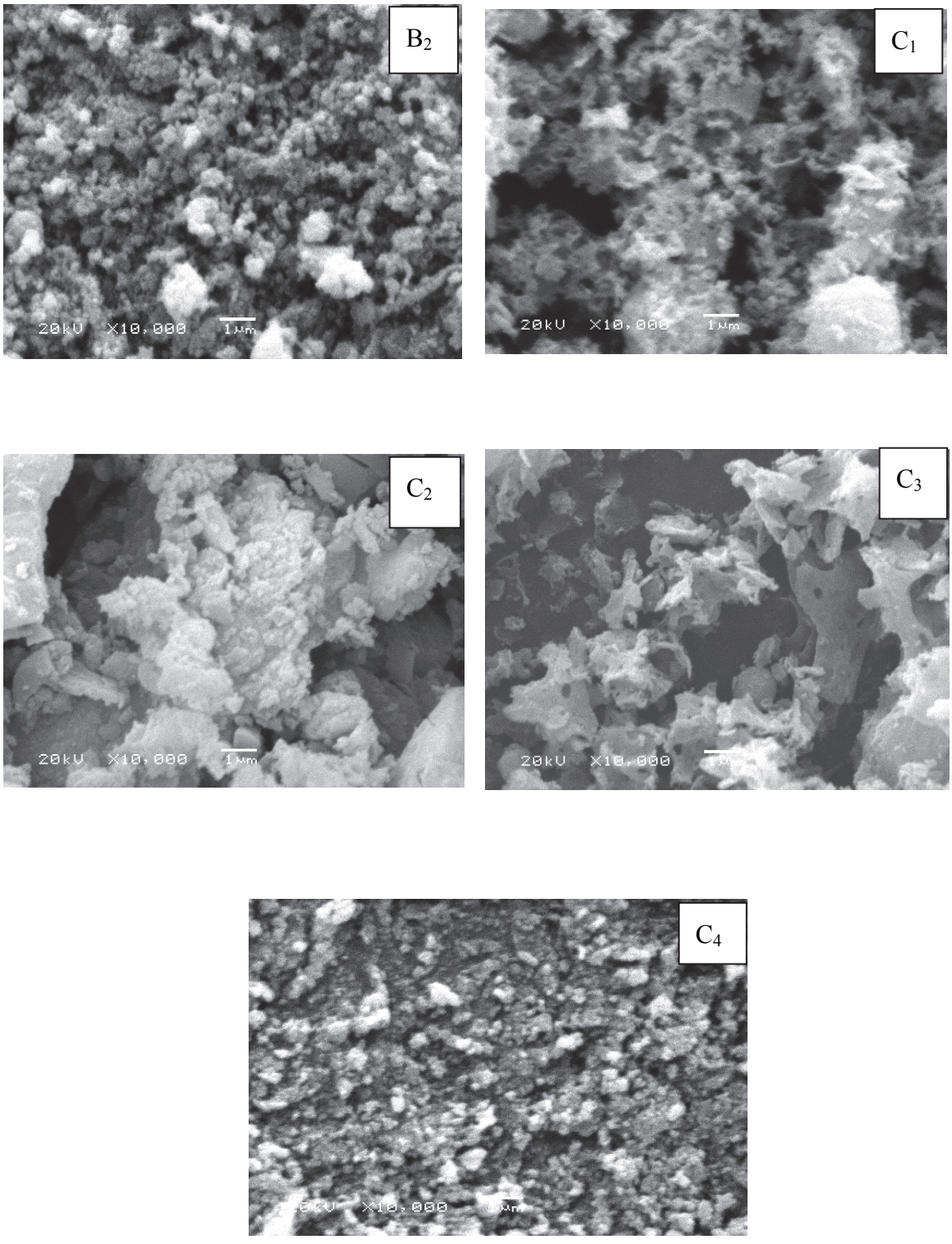

Figure 3: SEM Analysis of synthesized pure nano zinc oxide by both chemical and green synthesis methods: (A) chemical, (B_1) olive fresh, (B_2) guava fresh, (C_1) olive dry, (C_2) guava dry, (C_3) fig dry and (C_4) lemon dry.

3.3. Transmission electron microscopy (TEM)

In Press, Accepted Manuscript – Note to users

Figure 4 shows the TEM images of the ZnO nanoparticles synthesized using a zinc nitrate precursor by both chemical (A) and green synthesis methods using leave extracts via different Fresh and dry plant leave extracts of olive, guava, fig and lemon ($B_{1.1}$,$B_{1.2}$), B_2, C_1, C_2, C_3 and C_4). It can be observed that the particles have an almost spherical shape with small agglomeration in both chemical and green synthesis methods except green synthesis method using olive fresh plant leave extract the particles have nano rod with average nano rod size about 12-48 nm showen in **Figure 4** ($B_{1.1}$). The average particle size of ZnO in chemical synthesis method was found to be from 44 to 145 nm, When sodium hydroxide was replaced by different Fresh and dry plant leaves extracts of olive, guava, fig and lemon keeping the same procedure, the average size of particles reduced to 7.32-28 nm of the former ZnO particles, these results have good agreement with XRD results. A well dispersed rod like structure was observed with an average diameter of 8.9-21 nm was produced using olive fresh plant leave extract, which also relatively agree with the XRD results. It is clear from the TEM study that the average diameters of the ZnO NPs are almost the same if we use extracts from different Fresh and dry plant leaves of olive, guava, fig and lemon [26].

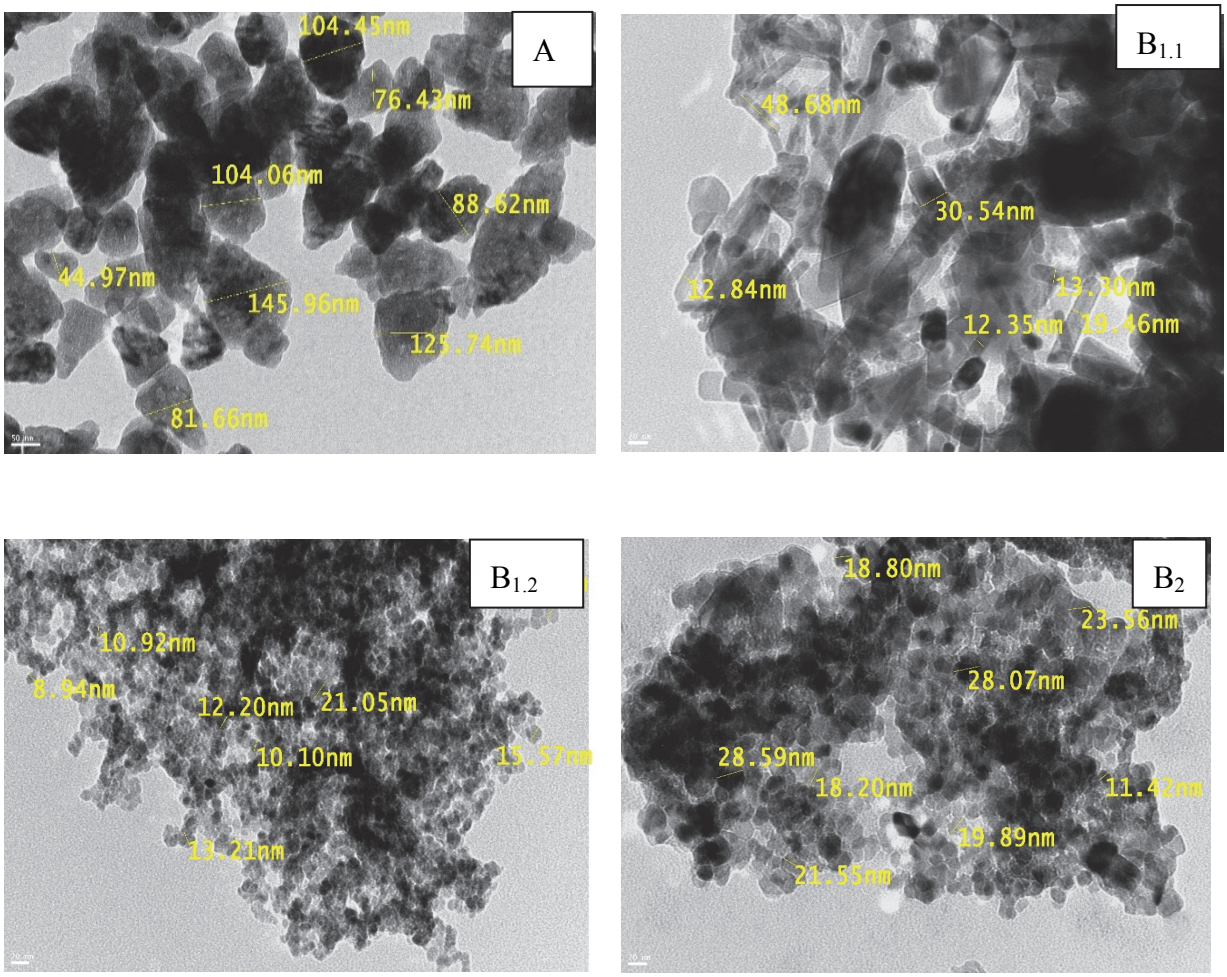

In Press, Accepted Manuscript – Note to users

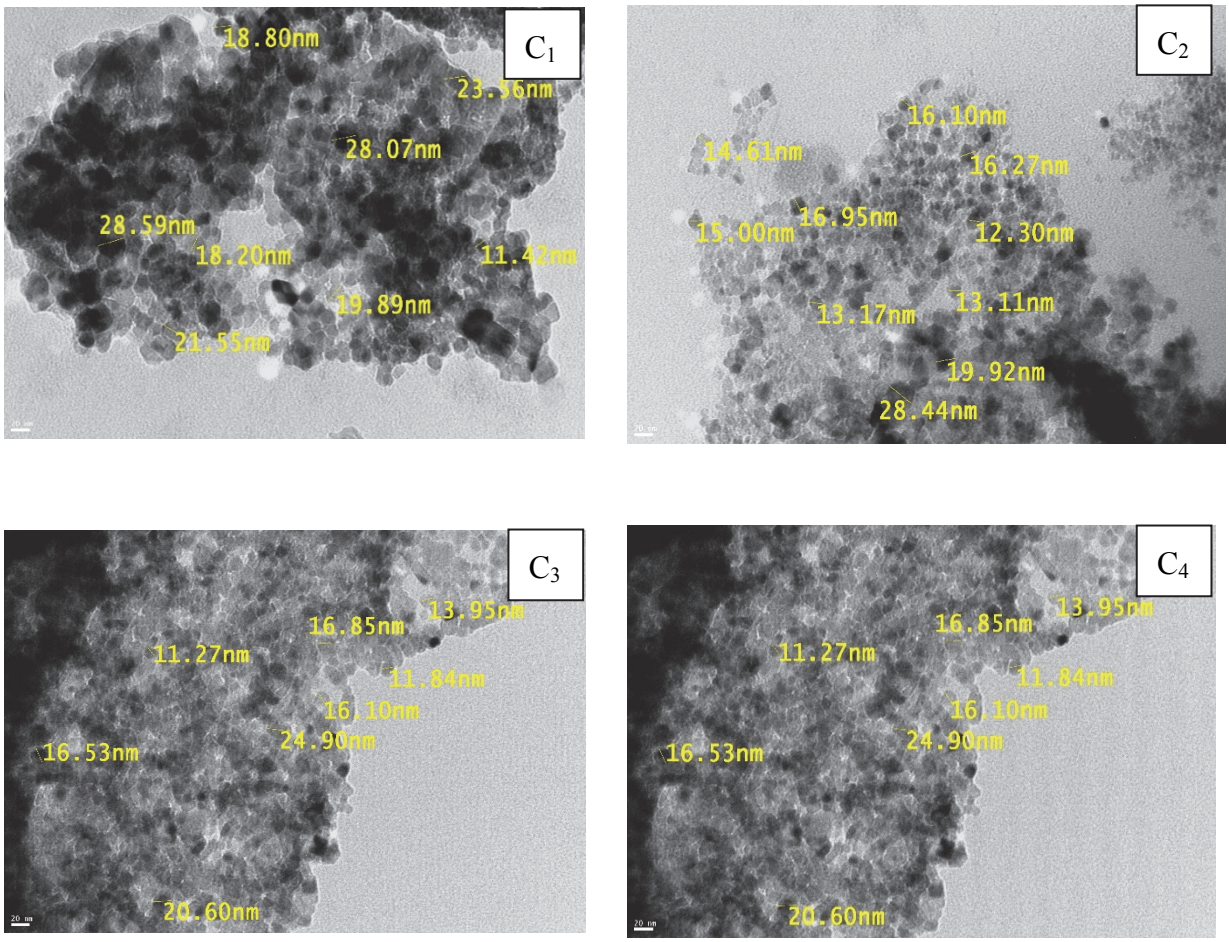

Figure 4 TEM images of the ZnO nanoparticles synthesized using both chemical and green synthesis methods: (A) chemical, ($B_{1.1}$, $B_{1.2}$) olive fresh, (B_2) guava fresh, (C_1) olive dry, (C_2) guava dry, (C_3) fig dry and (C_4) lemon dry.

3.4. FTIR spectroscopy

Figure 5 (A), (B_1) is recorded in the wavelength from 400cm^{-1} to 4000 cm^{-1} shows FTIR spectra of ZnO nanoparticles synthesized by both chemical **Figure 5** (A) and green **Figure 5** (B_1) methods using plant leave extracts. Generally, ZnO nanoparticles have characteristics absorption bands at region below 1000 cm^{-1} due to inter-atomic vibrations. The broad peak observed in chemical synthesis method at 3439.19 and 1103.32 cm^{-1} while in green synthesis method broad peak observed at 3398.89 and 1035.81 cm^{-1} correspond to O-H stretching band or may be due to the water adsorption on the metal surface. The peaks at 1639.55, 1635.69 cm^{-1}, 1456.30cm^{-1} and all bands at 449.43-557.45cm^{-1} is attributed to ZnO nanoparticles which are correspond to Zn-O stretching and deformation vibration, respectively. The broad peak at 1456.30cm^{-1} is due to the effect of polyphenols and natural pigments from plant leave extracts.

The broad peak at 3398.69 and 3439.19cm^{-1} are due to metal-oxygen (metal oxides) frequencies observed for the respective ZnO nanoparticles [7].

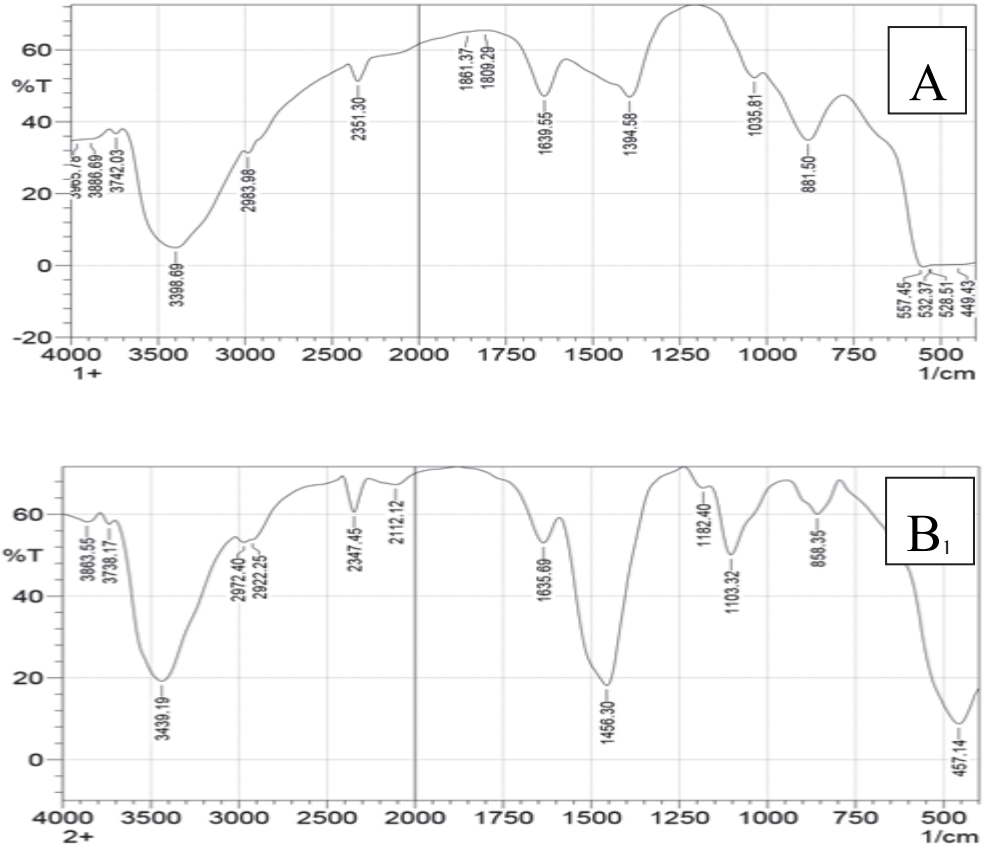

Figure 5 FTIR spectroscopy of chemical (A) and green (B_1) synthesis methods.

3.5. Thermal properties of the prepared materials (TGA)

Figure 6 (A, B_1 and B_3) showed the thermal decomposition behavior of the chemical and green synthesized ZnO nanoparticles over the studied temperature range 0 to 600^{o}C under N_2 atmosphere. With regard to chemical synthesized zinc oxide nanoparticles. The first degradation step that start at 25^{o}C and ended around 256^{o}C is attributed to the evaporation of surface adsorbed water. The second and third thermal degradation step start at 256^{o}C and ended around 599^{o}C may be caused by the decomposition of the condensation dehydration of the hydroxyls. The average samples weight losses at this temperature range for chemical synthesized ZnO nanoparticles not exceeded than 9.1% from the material weight showed in **Figure 6** (A). The first degradation step of green synthesized ZnO nanoparticles that calcinated in an air heated furnace at 500˚C for 2 hr before thermal decomposition, that start at 19^{o}C and ended around 200^{o}C is attributed to the removal of surface waste adsorbed onto zinc oxide. The second thermal degradation start at 200^{o}C and ended around 598^{o}C is attributed to the evaporation of surface adsorbed water and dehydration of the hydroxyls. The average samples

weight losses at this temperature range for green synthesized ZnO nanoparticles not exceeded than 2.2% from the material weight. This result clearly indicates that the obtained powder has extreme purity showed in **Figure 6** (B_1). On the other hand the first degradation step of green synthesized ZnO nanoparticles paste that non calcinated before thermal decomposition. That start at 38°C and ended around 93°C is attributed to the removal of surface waste adsorbed onto zinc oxide, then start at 93°C and ended around 177°C is attributed to the evaporation of surface adsorbed water, then start at 177 °C and ended around 282°C may be caused by the decomposition of the condensation dehydration of the hydroxyls. The last thermal degradation step start at 282°C and ended around 491°C might indicate the existence of organic material in small amounts. The average samples weight losses at this temperature range for green synthesized ZnO nanoparticles not exceeded than 51.6% from the material weight may be stand for the polyphenols or natural pigments from plant leaves extract degradation showed in **Figure. 6** (B_3) [27, 28].

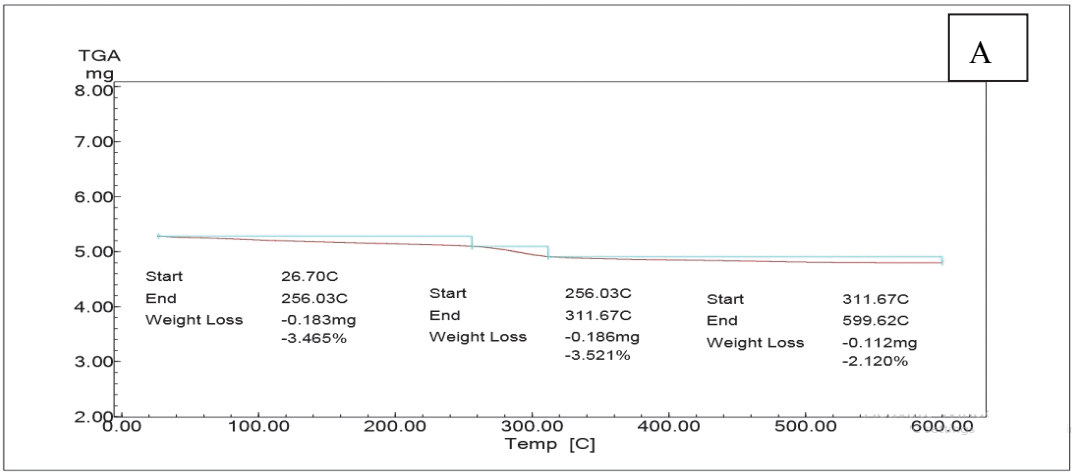

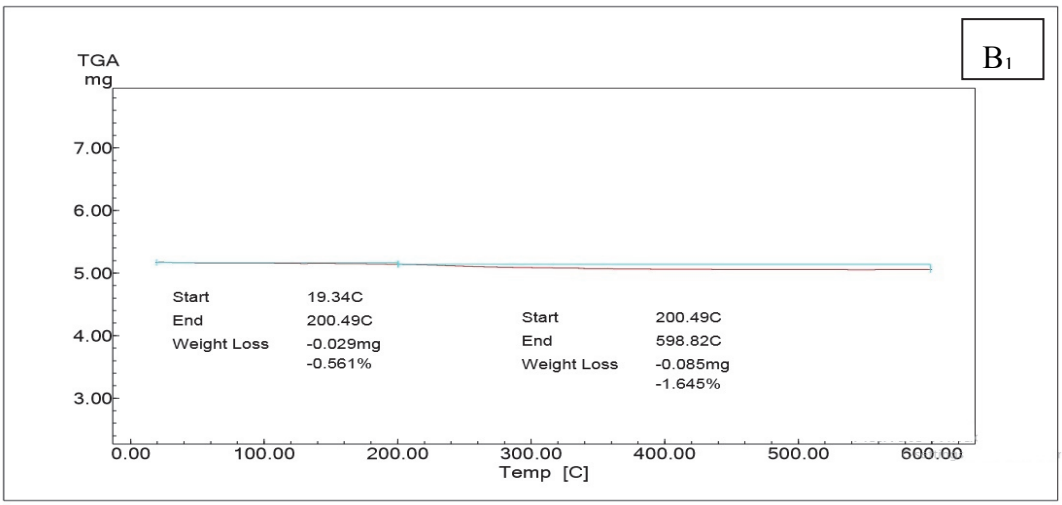

In Press, Accepted Manuscript – Note to users

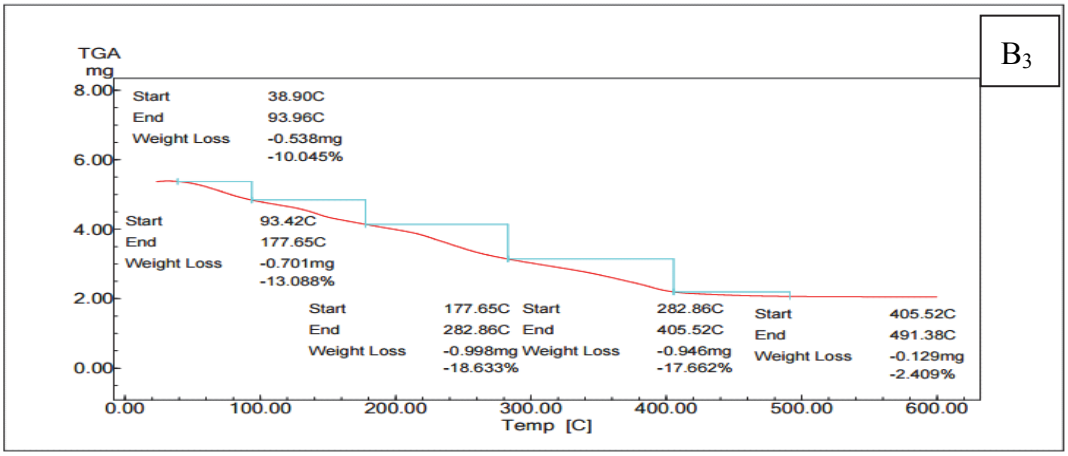

Figure. 6 Thermo gravimetric analysis (TGA) for ZnO nanoparticles: (A) chemical, (B_1) green synthesis methods calcinated ZnO nanoparticles at 500˚C for 2 hr and (B_3) green synthesis methods without calcination of ZnO paste.

3.6. Particle Size Analysis (PSA)

A laser diffraction method with a multiple scattering has been used to determine the particle size distribution of the powder. The particle size distribution curve for ZnO Nano-particles synthesized using both chemical and green synthesis methods are shown in **Figures 7** (A) and (B_1) respectively. The first peaks at **Figures** (7-A) and (8-B_1) appear at around 40 and 10 nm represent nano particles size diameter 9.2 in chemical synthesis method and 8.2 nm in green synthesis method. The presence of second peak has resulted in the average diameter of 526.6 nm in chemical synthesis method and 197.6 nm in green synthesis method. It corresponds with the crystallite size calculated from the SEM and XRD pattern and it is also clear that the average diameters and particle size of zinc oxide nanoparticles are smaller in green synthesis method compared with chemical synthesis method.

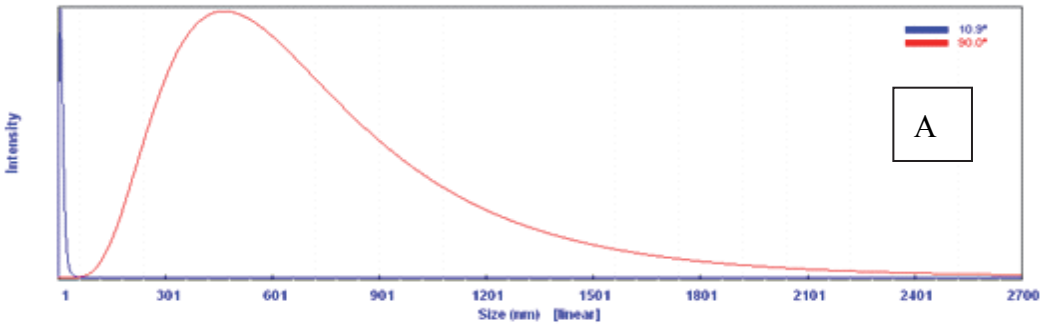

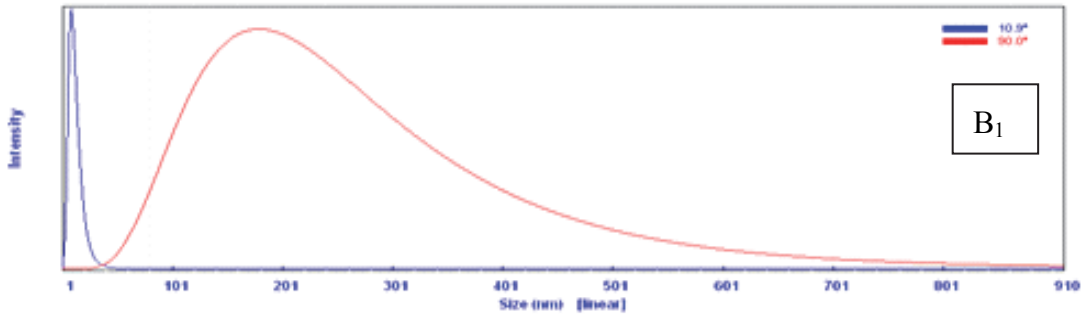

Figure 7 *Particle Size Analysis (PSA) for ZnO nanoparticles (A) chemical and (B_1) green synthesis methods.*

3.7. Assessment of the green synthetized ZnO-NPs for phenol sorption

The kinetic adsorption profile phenol onto ZnO-NPs was determined through variation the contact time from 0 min to 250 min at optimum concentration of phenol (5 ppm), a dose of adsorbent of (0.1 gm), and pH (8), temperature (25 °C) and agitation speed (300 rpm) as indicated in Figure 8. It was evident that the phenol adsorption onto ZnO-NPs was increased with increasing contact time. This result indicated that the high surface area of the prepared ZnO-NPs decreases the resistance of phenol diffusion that improves its mobility during adsorption process with time [29]. Moreover, Figure 5 indicates that the contact time has positive impact on phenol adsorption onto the ZnO-NPs. This behavior gives prediction that the adsorption process is mainly diffusion controlled. So, the adsorption affinity of phenol onto ZnO-NPs is increased with increasing the contact time until the equilibrium state [30].

Figure 8. Effect of contact time on phenol removal onto green synthetized ZnO-NPs.

4. Conclusions

In the present study it was found that the biosynthesis as green technology can be also good source for the synthesis of zinc oxide nanoparticles compared with chemical synthesis method. The bio-reduction of aqueous zinc ions using plant extracts of guava, olive, fig and lemon plant leaves has been demonstrated to produce ZnO nanoparticles. The green chemistry technique characterized by various advantages such as, simple to be scaled up, economic viability, easily available, familiar, and eco-friendly, etc... . The obtained ZnO was characterized using XRD, SEM, TEM, FT-IR, TGA and PSA analysis. It can be observed that ZnO nanoparticles have an almost spherical in shape with small agglomeration in both chemical and green synthesis methods excepting green synthesis method using olive extract the particles with average particle size about 8-28 nm corresponds with the crystallite size calculated from the SEM and XRD pattern. The thermal analysis results of ZnO nanoparticles produced from chemical and green synthesis indicated their thermal stability up to 600^{o}C. The green synthetized ZnO-NPs was evaluated for phenol decontamination from polluted wastewater. It showed maximum recorded phenol removal of 99.7% within 150 minutes using 0.1g ZnO-NPs. So, ZnO-NPs represent promising adsorbent material for phenol decontamination from polluted wastewater.

5. References

1. M.F. Elkady, H. Shokry Hassan. Curr. Nanosci. 11 (2015) 805.
2. E.T. Salem, R. A. Ismail, M.A. Fakhry, Y. Yusof, Int. J. Nanoelectronics and Materials 9 (2016) 111-122.
3. M.F. Elkady, H. Shokry Hassan. Nanoscale Res. Lett. 10 (2015) 1.
4. M. Shah, D. Fawcett, S. Sharma, S.K. Tripathy, G.E. Poinern, J. Materials. 8 (2015) 7278.
5. M. F. Elkady, H. Shokry Hassan, E.E. Hafez, and A. Fouad, Bioinorg. Chem. Appl. 2015 (2015) 20 pages, Article ID 536854.
6. C.N.R. Rao, S.R.C. Vivekchand, K. Biswasa, A. Govindaraj, J. Chem. Soc. Dalton Trans. 34 (2007) 3728.
7. M. Akl Awwad, B. Albiss, A.L. Ahmad, J. Adv. Mat. Lett. 5 (2014) 520.
8. O.J. Nava, P.A. Luque, C.M. Gómez-Gutiérrez, A.R. Vilchis-Nestor, A. Castro-Beltrán, M.L. MotaGonzález, A. Olivas, J. Mol. Struct. 12 (2016) 69.
9. K. Elumalai, S. Velmurugan, J. Appl. Surf. Sci. 345 (2015) 329.

10. Y.B. Saddeek, G.Y. Mohamed, H. Shokry Hassan, A.M.A. Mostafa, G. Abd elfadeel, J. Non-Cryst. Solids. 419 (2015) 110-117.
11. J. El Ghoul, C. Barthou, L. El Mir, J. Superlattices Microstruct. 51 (2012) 942.
12. D. Sarkar Tikku, S. Thapar, V. Srinivas, R.S. Khilar, J. Physicochem. Eng. 381 (2011) 123.
13. G. Bandekar, N.S. Rajurkar, I.S. Mulla, U.P. Mulik, D.P. Amalnerkar, P.V. Adhyapak, J. Appl. Nanosci. 4 (2014) 199.
14. E. R. Shaaban, M. El-Hagary, El Sayed Moustafa, H. Shokry Hassan, Yasser A. M. Ismail, M. Emam-Ismail, A. S. Ali, Appl. Phys. A 122 (2016) 1-10.
15. B.W. Chieng, Y.Y. Loo, J. Mater. Lett. 73 (2012) 78.
16. D. Ramimoghadam, M. Hussein and Y. Taufiq-Yap, J. Chem. Cent. 7 (2013)136.
17. R.P.P. Singh, I.S. Hudiara, S. Panday, P. Kumar, S.B. Rana, Int. J. Nanoelectronics and Materials 9 (2016) 1-8.
18. H. Shokry Hassan, M.F. Elkady, A.A. Farghali, Alaa Mohamed Salem, A.I. Abd El-Hamid, J. Taiwan Inst. Chem. Eng. 78 (2017) 307.
19. A. Sathya, and V. Ambikapathy, J. Plant. Sci. Res. 4 (2012) 486.
20. H. Michael Huang, S. Mao, H. Feick, H. Yan, Y. Wu, H. Kind, E. Weber, R. Russo, P. Yang, J. science. 292 (2001) 1897.
21. D. Gnanasangeetha, D. SaralaThambavani, J. Res. Material Sci. 7 (2013) 1.
22. Y.H. Tong, Y.C. Liu, S.X. Lu, L. Dong, S.J. Chen, Z.Y. Xiao, J. Sol-Gel .Sci .Tech. 30 (2004) 157.
23. Z. Tao, X. Yu, J. Liu, L. Yang, S. Yang, J. Alloys Compd. 459 (2008) 395.
24. R. zamari, A. Zakaria, H. Abbastar Ahangar, M. Darroudi, A. Zak and P.C. Gregor, J. Alloys Compd. 5 (2012) 41.
25. J. Yang, X. liu, L. Yang, y. wang, Y. zhang, J. Lang, M. Gao, M. Wei, J. Alloys Compd. 46 (2009) 743.
26. Q. Zhong, E. Matijevi´c, J. Mater. Chem. 6 (1996) 443.
27. H. Shokry Hassan, M.F. Elkady, E.E. Hafez, E. Salama, Nanoscience and Nanotechnology-Asia. 7 (2017) 62.
28. H. Shokry Hassan, M.F. Elkady, A. H. El-Shazly, H.S. Bamufleh. J. Nanomaterials. 2014 (2014) 14 pages, Article ID 967492.
29. E. R. Shaaban, M. El-Hagary, El Sayed Moustafa, H. Shokry Hassan, Yasser A. M. Ismail, M. Emam-Ismail, A. S. Ali, Appl. Phys. A 122 (2016) 1.

30. M. El kady, H. Shokry, H. Hamad, RSC Advances, 6 (2016), 82244.

E.T. Salem, R. A. Ismail, M.A. Fakhry, Y. Yusof, Int. J. Nanoelectronics and Materials 9 (2016) 111-122.

R.P.P. Singh, I.S. Hudiara, S. Panday, P. Kumar, S.B. Rana, Int. J. Nanoelectronics and Materials 9 (2016) 1-8.